2014

Progress on the Interaction Region Design and Detector Integration at Jlab's MEIC

V. S. Morozov

P. Brindza

A. Camsonne

Ya S. Derbenev

R. Ent

See next page for additional authors

Repository Citation

Morozov, V. S.; Brindza, P.; Camsonne, A.; Derbenev, Ya S.; Ent, R.; Gaskell, D.; Lin, F.; Nadel-Turonski, P.; Ungaro, M.; Zhang, Y.; Hyde, C. E.; Park, K.; Sullivan, M.; and Zhao, Z. W., "Progress on the Interaction Region Design and Detector Integration at Jlab's MEIC" (2014). *Physics Faculty Publications*. 276.
https://digitalcommons.odu.edu/physics_fac_pubs/276

Original Publication Citation

Morozov, V., Brindza, P., Camsonne, A., Derbenev, Y., Ent, R., Gaskell, D.... & Sullivan, M. (2014, July). Progress on the Interaction Region Design and Detector Integration at JLab's MEIC. In *Proceedings of the 5th International Particle Accelerator Conference (IPAC'14),* Dresden, Germany, June 15-20, 2014 (pp. 71-73). https://doi.org/10.18429/JACoW-IPAC2014-MOPRO005

Authors
V. S. Morozov, P. Brindza, A. Camsonne, Ya S. Derbenev, R. Ent, D. Gaskell, F. Lin, P. Nadel-Turonski, M. Ungaro, Y. Zhang, C. E. Hyde, K. Park, M. Sullivan, and Z. W. Zhao

PROGRESS ON THE INTERACTION REGION DESIGN AND DETECTOR INTEGRATION AT JLAB'S MEIC*

V.S. Morozov#, P. Brindza, A. Camsonne, Ya.S. Derbenev, R. Ent, D. Gaskell, F. Lin,
P. Nadel-Turonski, M. Ungaro, Y. Zhang, JLab, Newport News, VA 23606, USA
C.E. Hyde, K. Park, Old Dominion University, Norfolk, VA 23529, USA
M. Sullivan, SLAC, Menlo Park, CA 94025, USA
Z.W. Zhao, JLab & University of Virginia, Charlottesville, VA 22904, USA

Abstract

One of the unique features of JLab's Medium-energy Electron-Ion Collider (MEIC) is a full-acceptance detector with a dedicated, small-angle, high-resolution detection system, capable of covering a wide range of momenta (and charge-to-mass ratios) with respect to the original ion beam to enable access to new physics. We present an interaction region design developed with close integration of the detection and beam dynamical aspects. The dynamical aspect of the design rests on a symmetry-based concept for compensation of non-linear effects. The optics and geometry have been optimized to accommodate the detection requirements and to ensure the interaction region's modularity for ease of integration into the collider ring lattices. As a result, the design offers an excellent detector performance combined with the necessary provisions for non-linear dynamical optimization.

INTRODUCTION

The Electron Ion Collider (EIC) will be a next-generation facility for the study of the strong interaction (QCD). JLab's MEIC [1] is designed for high luminosities of up to 10^{34} cm^{-2}s^{-1}. MEIC's primary detector is unique in its ability to provide essentially full acceptance to all fragments produced in collisions. The detector design relies on a number of features, such as a 50 mrad beam crossing angle, large-aperture ion and electron final focusing quads and spectrometer dipoles as well as a large machine-element-free detection space downstream of the final focusing quads [2,3].

Two detector regions have been integrated into the collider ring lattices with necessary optical and geometric matching as illustrated in Fig. 1. The detectors are placed far from the electron arc exits to minimize the synchrotron radiation background and close to the ion arc exits to minimize the hadronic background due to the ion beam scattering on the residual gas. The two detector region designs are identical at the moment but can be customized in a straightforward way in the future to complement each other's functionality.

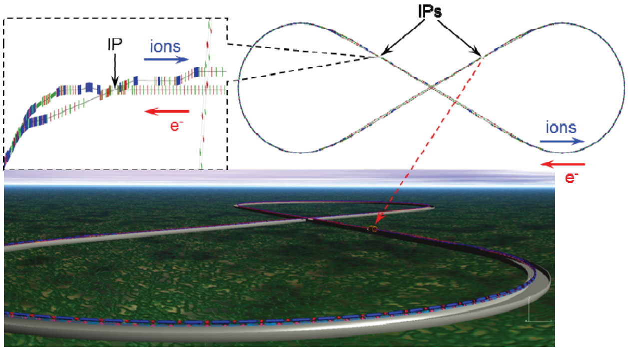

Figure 1: Collider rings' layout, 3D view and IP locations.

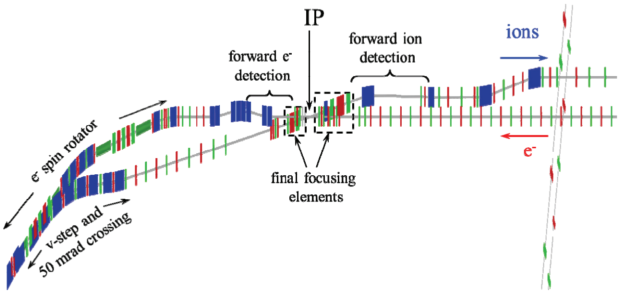

Figure 2: Detector region layout.

DETECTOR REGION

Geometric Configuration

The relatively large 50 mrad crossing angle allows quick separation of the two colliding beams near an interaction point (IP) for avoiding undesirable parasitic collisions of 40-cm-spaced electron and ion bunches as well as making sufficient space for placement of interaction region magnets. It also moves the spot of poor resolution along the solenoid axis into the periphery and minimizes the shadow of the electron final focusing quadrupoles. On the other hand, a non-zero crossing angle requires crab tilt of the colliding bunches to restore their head-on collisions and preserve the luminosity.

Figure 2 shows an expanded view of the detector region layout. The end section of the ion arc upstream of the IP is shaped to produce a net 50 mrad horizontal angle between the ion and electron beams while the ion beam line segment downstream of the IP is designed to make a 2 m transverse separation between the ion and electron beams. The electron detector region has no overall bend or shift.

---

*Authored by Jefferson Science Associates, LLC under U.S. DOE Contract No. DE-AC05-06OR23177 and DE-AC02-06CH11357. The U.S. Government retains a non-exclusive, paid-up, irrevocable, world-wide license to publish or reproduce this manuscript for U.S. Government purposes.

#morozov@jlab.org

This makes the collider ring geometry somewhat independent from the detector region design and simplifies its optimization [3].

Linear Optics Design

Due to kinematic considerations, more detector space is needed along the ion beam direction downstream of the IP than in the upstream direction. Consequently, the upstream ion Final Focusing Block (FFB) is placed closer to the IP (at a distance of 3.5 m) than the downstream one (at a distance of 7 m) yielding an asymmetric detector region design. Each ion FFB is a quad triplet allowing for a more flexible control of the beta functions. Electron FFBs are based on quad triplets but include additional permanent-magnet quads placed at the front of the FFBs. The permanent-magnet quads have a small size and can be placed closer to the IP. Change of their focusing strength with energy is compensated by adjusting the regular electro-magnet FFB quads. The electron FFBs on both sides are placed 3 m away from the IP. The downstream ion and electron final focusing quads are designed with large apertures for forward detection and are followed by spectrometer dipoles. Additionally, there is a weak spectrometer dipole in front of the downstream ion FFB. Such a design shown in Fig. 3 satisfies the detector requirements while minimizing the chromatic contribution of both the ion and electron FFBs.

Sufficient machine-element-free space is reserved beyond the downstream FFBs and spectrometer dipoles for detection purposes. Both the ion and electron beams are focused again towards the end of this element-free space to allow closer placement of the detectors, which, in combination with relatively large dispersion at those points, enhances the forward detector's momentum resolution. The dispersion generated by the spectrometer dipoles is suppressed on the ion side by a specially designed section, which also controls the beam line geometry, while on the electron side the dispersion suppression is done by a simple dipole chicane whose parameters are chosen to avoid a significant impact on the electron equilibrium emittances. The optics of the ion and electron detector regions are shown in Figs. 4 and 5, respectively [3].

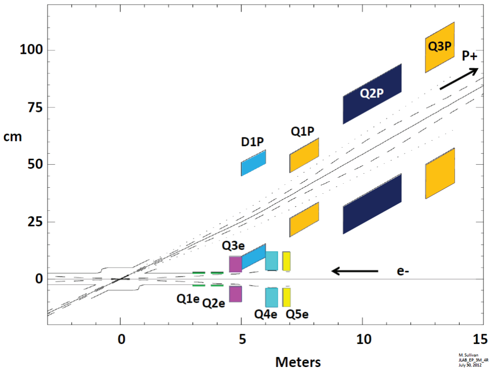

Figure 3: Layout of the detector region magnets in the forward ion direction.

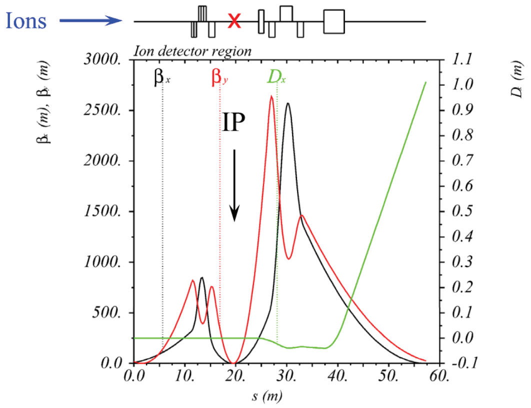

Figure 4: Optics of the ion detector region.

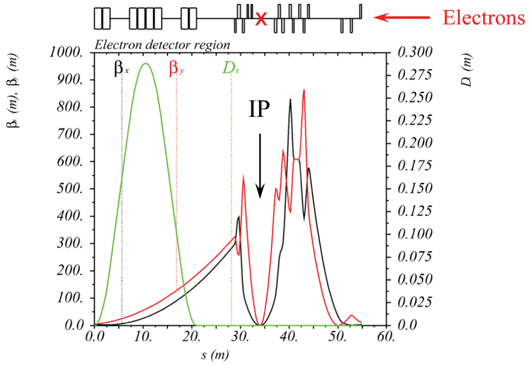

Figure 5: Optics of the electron detector region.

Non-Linear Dynamics Considerations

Due to the strong beam focusing at the IPs, the chromatic effect of the FFBs in both the ion and electron collider rings is very significant and requires proper compensation. MEIC employs a local compensation approach where dedicated Chromaticity Compensation Blocks (CCBs) induce momentum-angle correlations in the passing beam such that they cancel the chromatic kick of the FFBs [4,5]. Each CCB is a symmetric structure of magnetic elements including sextupoles that is designed with certain symmetries of the orbital motion. These symmetries allow the CCBs to provide the necessary chromatic compensation without generating other, undesirable significant non-linear effects. In the ion collider ring, the CCBs are placed in the arcs while, in the electron collider ring, due to a special design taking into account the electron emittance considerations, the CCBs have zero net bend and are placed in the straights. Initial simulation using this concept yielded encouraging results. Detailed studies and optimization of the non-linear dynamics are underway.

Detector Simulations

Figure 6 shows a 3D view of the detector and adjacent machine elements modeled in GEANT4 [6,7]. The detector's angular and momentum acceptance and its resolution have been simulated using this model and found to satisfy all of the physics requirements [2]. In particular, one of the important features of this design is illustrated in Fig. 6: neutral particles originating at the IP pass through the apertures of the ion ring's downstream machine elements and get sufficiently separated from both beams for detection with zero-degree calorimetry.

Figure 7 shows an example of a detector simulation involving the Deep Virtual Compton Scattering (DVCS) process [7,8]. The recoil protons produced in the process are detected by the forward detectors. The proton momenta are close to the 100 GeV/c beam momentum and their initial scattering angles are up to 10 mrad. Note that in this case the detector's acceptance is only limited by the size of the region near the beam itself (the beam stay-clear) where detectors cannot be placed.

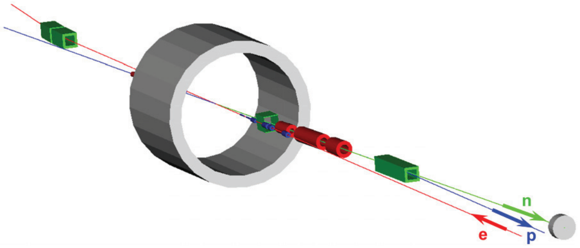

Figure 6: 3D view of the detector model.

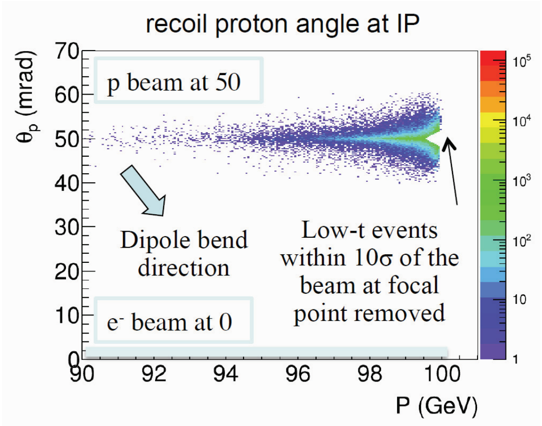

Figure 7: Simulation of recoil proton detection in the DVCS process.

Detector Solenoid

Two existing, nearly identical solenoids (CLEO and BaBar) would be suitable for use in the EIC detectors. However, an interesting option would be to instrument one of the IPs using a detector based on a dual-solenoid illustrated in Fig. 8, where the field in the outer one cancels the inner one [9]. Aside from providing a light-weight option with low fringe fields, a new dual-solenoid could also offers higher field (2-3 T vs 1.5 T of the existing magnets). More importantly, however, the active field shaping (using coils in the endcaps and elsewhere) can create a field allowing optimal performance of the various subsystems (tracking, PID, etc). Furthermore, its spacious endcaps allow more solid angle with high-precision forward detectors for a given solenoid size and provide easy access to the detectors located there.

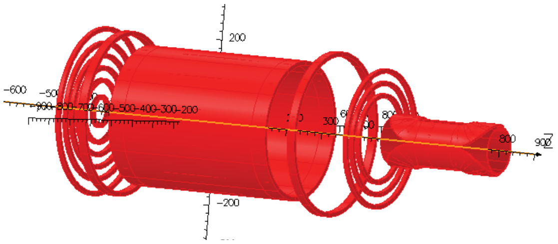

Figure 8: Detector dual-solenoid design.

Electron Polarimetry Using Low-Q^2 Chicane

One of the major assets of MEIC is the polarization of both ion and electron beams. As far as the electron beam is concerned, there will be two helicity states in the ring and the Compton process allows one to monitor their polarization non-invasively and continuously by intersecting the electron beam with a polarized laser beam usually in a magnetic chicane. A photon is emitted almost collinearly to the beam and continues straight while the electron beam follows the path of the chicane allowing for detection of the photon in a calorimeter. At the same time, the Compton electron, which lost energy, is deflected out of the beam and can be detected using a tracking detector as depicted in Fig. 9. By measuring the Compton spin asymmetry, one can measure the beam polarization. We are currently studying the possibility of placing a Compton polarimeter in the low-Q^2 chicane to take advantage of its magnets for the polarimetry. We are considering the options of strip detectors in vacuum or in roman pots. At the MEIC energies and electron beam currents, we are aiming to reach 1% accuracy.

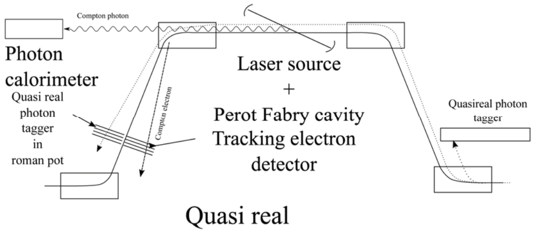

Figure 9: Compton polarimeter schematic.

REFERENCES

[1] S. Abeyratne et al., "Science requirements and conceptual design for a polarized medium energy electron-ion collider at Jefferson lab", edited by Y. Zhang and J. Bisognano, arXiv:1209.0757 (2012).
[2] V.S. Morozov et al., IPAC'12, TUPPR080, p. 2011.
[3] F. Lin et al., PAC'13, TUPAC28, p. 508.
[4] F. Lin et al., IPAC'12, TUPPC099, p. 1389.
[5] V.S. Morozov et al., PRST-AB 16, 011004 (2013).
[6] G4beamline, http://g4beamline.muonsinc.com
[7] Simulation framework, GEMC, http://gemc.jlab.org
[8] MILOU DVCS event generator, https://wiki.bnl.gov/eic/index.php/MILOU
[9] M. Wake et al., Fermilab Tech. Report, TD-09-030 (2009).